

Canine Model of Convection-Enhanced Delivery of Cetuximab-Conjugated Iron-Oxide Nanoparticles Monitored With Magnetic Resonance Imaging

Simon Platt, BVM&S, MRCVS, Edjah Nduom, MD, Marc Kent, DVM, Courtenay Freeman, DVM, Revaz Machaidze, BS, Milota Kaluzova, PhD, Liya Wang, MD, Hui Mao, PhD, and Costas G. Hadjipanayis, MD, PhD

Convection-enhanced delivery (CED) of therapeutic agents has been used in multiple human clinical trials to determine therapeutic efficacy against malignant brain tumors.^{1,2} CED has been designed to infuse agents intratumorally and into the surrounding brain parenchyma, bypassing the blood-brain barrier and avoiding nonspecific uptake.³ The positive pressure gradient established during CED permits fluid convection and enhances the distribution of molecules into brain.⁴ Therapeutic agents can be delivered into the brain by CED in high concentrations without the toxicity to normal tissue and organs commonly associated with systemic delivery.⁵ The use of CED can also allow therapeutic targeting of infiltrating cancer cells in the normal brain, a major cause of brain tumor recurrence after surgery.

The lack of noninvasive monitoring of CED in the brain for agent distribution and tumor targeting is the single largest impediment to this delivery strategy. Ineffective drug distribution is a major criticism of CED that may compromise malignant brain tumor targeting and therapy.⁶ Agent surface properties (cationic charge), large hydrodynamic size, catheter positioning, and high interstitial tumor pressures can compromise agent distribution.^{4,6-10} Visualizing the distribution of infused agents is necessary to ensure accurate delivery into target sites and provides feedback on catheter placement and control of agent delivery.^{11,12} Previous studies have radiolabeled their therapeutic agent, co-infused their agent with radiolabeled albumin (¹²³I-labeled albumin), or used liposomes containing a magnetic resonance imaging (MRI) contrast agent (eg, gadoteridol) for real-time CED imaging.¹³⁻¹⁶ Radiolabeling of therapeutic agents relies on low-resolution single-photon emission computerized tomography for agent imaging and raises concerns of using radioactive materials with CED. Coinfusion of imaging agents with different size and surface properties may not accurately depict actual therapeutic agent distribution and cannot be performed over time.

Recently, CED of magnetic iron-oxide nanoparticles (IONPs; core size, 10 nm) conjugated to an epidermal growth factor receptor (EGFR) deletion mutant (EGFRvIII) antibody has been reported for the therapeutic targeting of human glioblastoma multiforme (GBM) in a rodent model.¹⁷ Because of their unique magnetic properties, IONPs serve as a strong MRI contrast agent, enabling monitoring of CED of IONPs directly by MRI for distribution studies in the brain.¹⁸ Distribution of the EGFRvIII antibody-conjugated IONPs within the GBM xenografts was initially observed, and the dispersion of the nanoparticles intratumorally and peritumorally in the brain occurred for days after CED. This study demonstrated the feasibility of CED for MRI-assisted effective delivery of IONPs within brain tumors and the infiltrating cancer cells beyond the tumor mass responsible for tumor recurrence.

Translation of this promising imaging-guided therapeutic approach into human clinical trials requires demonstration of the safety and efficacy of EGFR antibody-conjugated IONP treatment in a larger animal model. Use of a canine model permits feasibility and toxicity evaluation on a scale relevant to human patients. Furthermore, canines with spontaneous gliomas may serve as the most relevant model for testing the efficacy and treatment responses of therapeutic agents because canine tumors present features similar to human glioblastomas. Similar tumor infiltration into the normal brain, clinical MRI features, and tumor cell EGFR overexpression and signaling alterations have been reported in spontaneous canine gliomas.¹⁹⁻²¹

In this work, we report our investigation of MRI-assisted CED of IONPs conjugated to cetuximab, a monoclonal antibody specific to the wild-type EGFR that cross-reacts with the EGFRvIII deletion mutant, in a canine model. Volume of distribution (V_D), dispersion (V_{DI}), clearance, and toxicity studies were performed in healthy canines. We demonstrated the feasibility and safety for CED of IONPs to clinically significant areas of the canine brain. Furthermore, the procedure can be monitored directly with MRI.

PATIENTS AND METHODS

Experimental Animals

Eight healthy beagle dogs (4 males and 4 females) were used for the experimental protocol. All canine studies were performed at the University of Georgia College of Veterinary Medicine, an American Veterinary Medical Association-accredited and -approved college of veterinary medicine. The experimental protocol was reviewed and approved by the Institutional Animal Care and Use Committee at the University of Georgia College of Veterinary Medicine. All canines were housed individually in concrete runs and maintained on a 12-hour light/dark cycle with a room temperature of 20°C to 22°C. A standard commercial maintenance dry food diet was provided on a daily basis with water provided ad libitum. All animals underwent complete physical and neurological examinations before the procedure and daily thereafter until completion of the study. Animal weights were also documented.

Bioconjugated Cetuximab-IONPs

Clinical grade cetuximab (Imclone, Inc) was obtained from the Winship Cancer Institute of Emory University for conjugation to the IONPs (Figure 1). Amphiphilic triblock copolymer-coated IONPs (core size, 10 nm) were obtained from Ocean Nanotech, Inc (Figure 1). A 1:1 antibody to IONP conjugation was performed. Briefly, activation of the carboxyl groups on the IONPs was performed for conjugation of the cetuximab antibody after addition of an activation buffer, ethyl dimethylaminopropyl carbodiimide (EDC) and sulfo-NHS. The EDC/NHS solution was mixed vigorously with the IONPs at 25°C for 15 minutes. Excess EDC and sulfo-NHS were removed from the activated nanoparticles by 3 rounds of centrifugation (1000g) and resuspension in phosphate-buffered saline with Nanosep 10K MWCO OMEGA membrane (Pall Life Sciences). The IONPs with activated carboxyl groups were then reacted with cetuximab (50 µL at 2 mg/mL) at 25°C for 2 hours, and the reaction mixture was stored at 4°C overnight. Excess antibody was removed by 3 rounds of centrifugation and resuspension in phosphate-buffered saline with 100K

MWCO OMEGA membranes. Conjugation efficiency was confirmed by mobility shift in 1% agarose gel and was visualized by staining with 0.25% Coomassie Brilliant Blue in 45% methanol/10% acetic acid for 1 hour and destaining in 30% methanol/10% acetic acid overnight (Figure 1). Cetuximab-IONPs or IONPs were suspended in phosphate-buffered saline, and a concentration of 0.2 mg/mL was used for all canine CED studies.

Canine IONP CED Studies

Two groups of healthy dogs underwent CED of free IONPs (group 1; n = 4) or bioconjugated cetuximab-IONPs (group 2; n = 4) after placement of a single closed-tip catheter (Hermetic Catheter, Integra NeuroSciences) through a 3- to 5-mm right frontal burr hole approximately 1.5 to 2 cm into the frontal lobe after general anesthesia (Figure 2). Each catheter was tunneled under the skin and connected to an external programmable reservoir infusion pump (Medtronic Synchromed II, Medtronic Inc) that was strapped to each animal's head (Figure 2). Each pump was filled with either free IONPs or cetuximab-IONPs. Infusions were performed after programming of the external reservoir pump (Medtronic Synchromed II) with a handheld device. Animals did not require anesthesia for their CED procedures. The CED parameters of infusion rate (I_R) and volume (V_i) were programmed. Animals underwent IONP CED at a rate of 0.5, 1.0, 3.0, or 5.0 µL/min for 1, 6, 12, or 24 hours. V_i ranged from 180 to 720 µL.

IONP MRI Distribution Studies

Brain MRI scans were performed on all dogs before and within 12 hours after their CED procedure. Group 1 dogs underwent a brain MRI scan 7 days after CED for initial feasibility studies. Group 2 animals underwent MRI scans at 5 and 30 days after CED to determine IONP V_D , V_{DI} , and clearance with lower infusion rates. All MRI experiments were done with a whole-body 3-T MRI scanner (Signa HDx). Under general anesthesia, dogs were placed in sternal recumbency. The head was immobilized in the single channel extremity coil and positioned in the isocenter of the magnet. Whole-brain scans were performed with T1-weighted spin-echo sequence, T2-weighted

FIGURE 1. Cetuximab-conjugated iron-oxide nanoparticles (IONPs). A, an IONP (red; core size, 10 nm) coated with a bio-compatible amphiphilic triblock copolymer¹⁷ bioconjugated to the epidermal growth factor receptor monoclonal antibody cetuximab is shown. Bioconjugation of cetuximab is performed to the -COOH of the polymer coating. B, agarose gel electrophoresis confirming IONP bioconjugation to cetuximab (asterisk). Free IONPs are shown on the left.

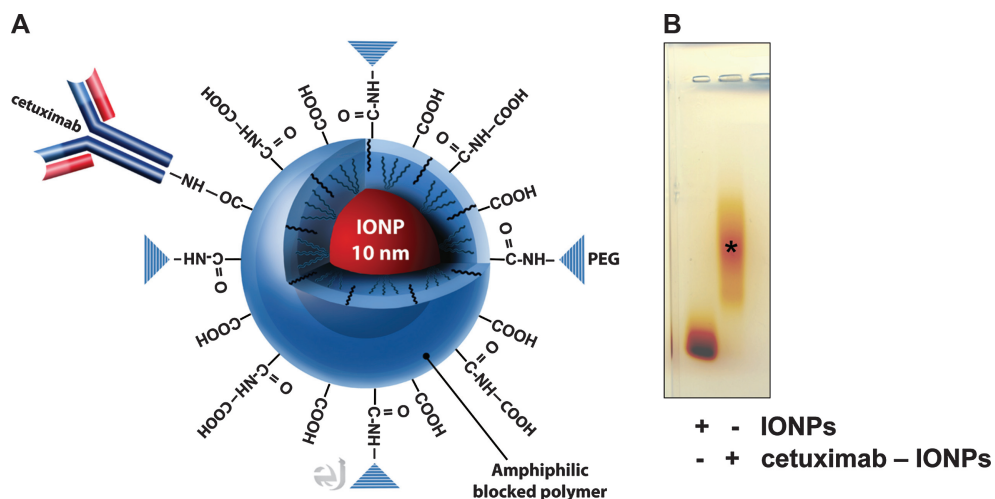


FIGURE 2. Canine iron-oxide nanoparticle (IONP) convection-enhanced delivery (CED) setup. A, a single CED catheter is tunneled subcutaneously through the scalp after being placed 1 to 2 cm into the right frontal lobe through a burr hole. B, strapping of an external programmable reservoir infusion pump to a canine's head for IONP CED.



fast spin-echo sequence, T2-weighted flow-attenuated inversion recovery sequence, and 3-dimensional gradient echo sequence before and after IONP CED. Because the size of the canine brain approaches that of the human brain, MRI parameters selected for each canine were slightly modified from those of the brain MRI protocol used in human patients at Emory University. A field of view of 20 cm, matrix of 256 by 256, and slice thickness of 4 mm (no gap) were used in the scan sequences. The scans were performed in the coronal sections.

Region-of-interest analysis was used to determine the V_D of IONPs at different time points after CED. Because IONPs induce hypointensity (signal drop) with T2-weighted imaging (T2WI), the boundaries of each region of interest can be drawn manually on each T2WI slice based on the 10% signal loss in each voxel where IONPs were infused. The number of voxels selected based on this criteria were summed from each slice showing IONP-induced contrast change. A V_D calculation will be the sum of voxels showing signal drops, ie, $V_D = N_s \times S \times R$, where N_s is number of voxel in each slice that have defined signal drops, S is number of slices where voxels are selected, R is in plane resolution in millimeters. The V_{DI} of the IONPs was determined by the difference in V_D measurements within 12 hours after CED and each time point after.

Hematologic and Cerebrospinal Fluid Analyses

Complete blood counts and serum biochemical analyses were performed on all canines 7 and 30 days after CED. Blood samples were collected by jugular puncture. Cerebrospinal fluid analysis was performed 7 days after CED. Cerebrospinal fluid was obtained by cerebellomedullary cisternal puncture with the animals under general anesthesia.

Brain Histological Analysis

Brains were harvested from all the animals 30 days after their CED procedure and immersed in 10% buffered formalin

for 10 days before sectioning and histopathological analysis. Representative sections of the brain were made at each site of CED catheter placement. Sections 5 μ m thick were processed for routine hematoxylin and eosin staining and for Perl blue staining for iron.

RESULTS

Initial CED and Distribution of IONPs in the Canine Brain

Distribution of the IONPs in the canine brain was achieved for the first time by CED. Direct imaging of delivery of IONPs and intracranial distribution of nanoparticles by T2WI was possible. Both T1-weighted imaging and T2WI confirmed no presence of hemorrhage after each CED procedure.

Group 1 ($n = 4$) received free IONPs (0.2 mg/mL) for 60 minutes at either 3 or 5 μ L/min ($V_i = 180 \mu$ L and $I_R = 3.0 \mu$ L/min rate in dogs 1 and 2; $V_i = 300 \mu$ L and $I_R = 5.0 \mu$ L/min rate in dogs 3 and 4; Figure 3). One dog in group 1 (dog 2) was found to have intraventricular distribution of IONPs caused by catheter entry into the ventricle (Figure 3) that was not visualized by MRI 7 days later. One dog in group 2 (dog 8) was found to have subarachnoid distribution of IONPs because the catheter had not penetrated the brain. Infusate leak-back along the catheter was found at the infusion rates of 1, 3, and 5.0 μ L/min (Figure 3).

Group 2 (dogs 5-8) underwent CED of bioconjugated cetuximab-IONPs (0.2 mg/mL) at 0.5 or 1.0 μ L/min for 6, 12, or 24 hours ($V_i = 360 \mu$ L and $I_R = 0.5 \mu$ L/min rate [12 hours] in dog 5; $V_i = 720 \mu$ L and $I_R = 0.5 \mu$ L/min rate [24 hours] in dog 6; $V_i = 360 \mu$ L and $I_R = 1.0 \mu$ L/min rate [6 hours] in dog 7; $V_i = 720 \mu$ L and $I_R = 1.0 \mu$ L/min rate [12 hours] in dog 8; Figure 4).

Use of a slower I_R at 0.5 μ L/min provided a more uniform distribution of IONPs and low infusate leak-back, as indicated by the T2WI in Figure 4. Semiquantitative

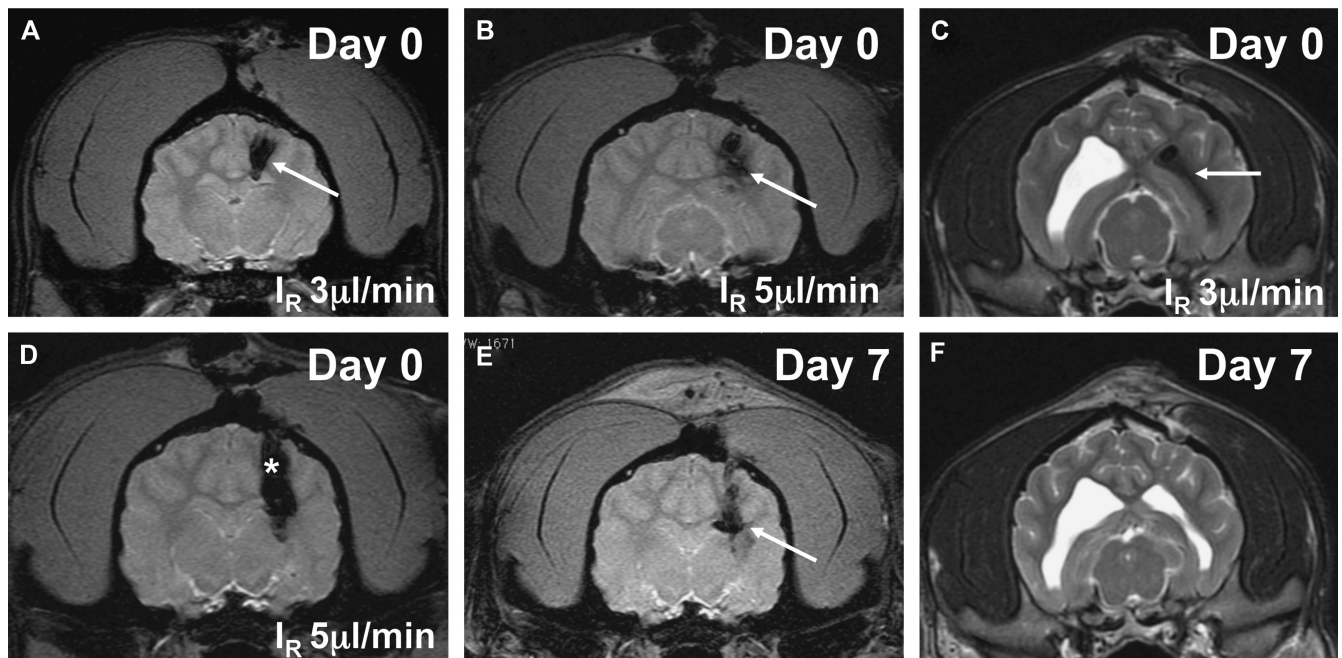


FIGURE 3. Initial free iron-oxide nanoparticle (IONP) convection-enhanced delivery (CED) studies in the healthy canine brain (group 1; 60-minute infusions), T2-weighted imaging (including gradient echo), and IONP magnetic resonance imaging contrast effect (shown by arrows). A, IONP CED (V_i , 180 μ L; I_R , 3 μ L/min) at day 0. B, IONP CED (V_i , 300 μ L; I_R , 5 μ L/min) at day 0. C, intraventricular placement of IONPs after CED. D, leak-back of IONPs along catheter (asterisk) is shown at the higher I_R (5 μ L/min). E, presence of intracerebral IONPs 7 days after CED. F, clearance of intraventricular IONPs 7 days after CED.

measurement of areas where IONP induced MRI contrast changes allowed us to determine that V_D is linearly proportional to the V_I (Figure 5). The V_D was greatest at 0.5 μ L/min for 24 hours (289 mm^3).

Dispersion of the cetuximab-IONPs was found 5 days after CED in group 2 (Figure 5). Greater dispersion was found with use of the slower I_R (0.5 μ L/min; V_{DI} , 35 mm^3) compared with the I_R of 1.0 μ L/min (V_{DI} , 7 mm^3 ; Figure 5).

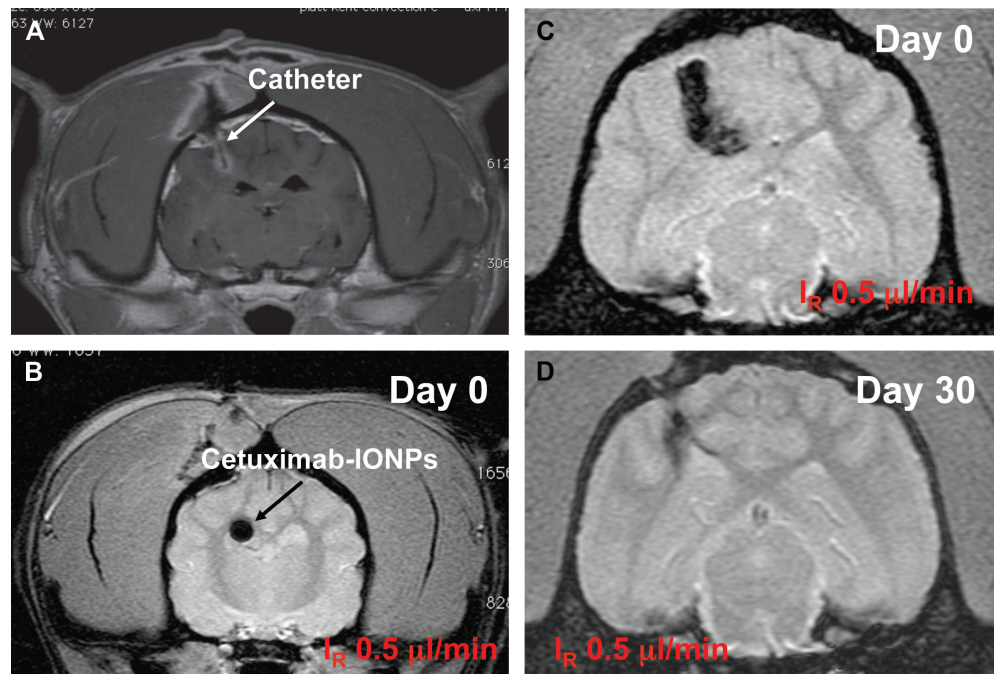


FIGURE 4. Magnetic resonance imaging-guided cetuximab-iron-oxide nanoparticle (IONP) convection-enhanced delivery (CED) in the canine brain (group 2). A, T1-weighted image confirming catheter positioning. B, T2-weighted image showing uniform distribution of IONPs (black arrow) at the lower infusion rate (I_R , 0.5 μ L/min) for 12 hours (B) and greater distribution at 24 hours (C). Loss of T2 hypointensity (D) 30 days after CED.

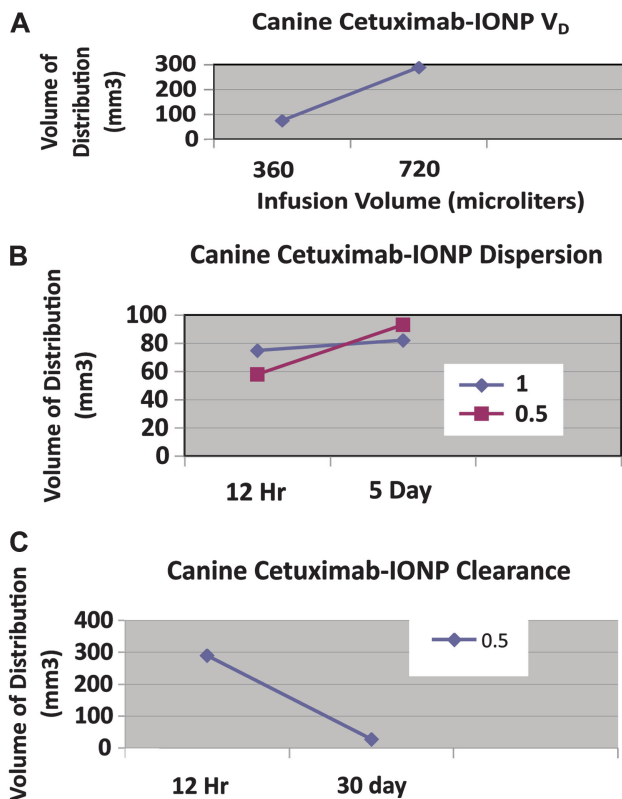


FIGURE 5. Cetuximab–iron-oxide nanoparticle (IONP) convection-enhanced delivery (CED) volume of distribution, dispersion, and clearance in the canine brain (group 2). A, IONP volume of distribution (V_D) after CED was determined by T2 contrast (signal drop) present on T2-weighted imaging (T2WI). V_D was linearly proportional to the infusion volume (V_I). B, initial IONP V_D after CED was determined at 12 hours on day 0 with a CED infusion rate (I_R) of 0.5 or 1.0 $\mu\text{L}/\text{min}$. The V_D was determined 5 days after CED, confirming dispersion of the bioconjugated IONPs at both I_R values. Greater IONP dispersion was found at the 0.5- $\mu\text{L}/\text{min}$ rate. C, clearance of IONPs was determined by T2WI V_D comparison at 12 hours and 30 days after CED of IONPs (0.5 $\mu\text{L}/\text{min}$ for 24 hours). T2 contrast is almost completely gone at 30 days.

Toxicity and Clearance of IONPs From the Canine Brain After CED

All dogs showed no signs of toxicity after IONP CED. No neurological deficits were noted in any of the dogs during the 30-day observation period after their CED procedure, and all dogs maintained their normal weight. All dogs showed no abnormalities on cerebrospinal fluid, hematology, and serum biochemistry analyses 7 days after CED. Hematology and serum biochemistry remained normal at 30 days after CED.

For IONP clearance studies, dogs in group 2 underwent an additional MRI scan at 30 days. IONP-associated contrast was found on T2WI at 30 days, but at a much smaller volume, confirming bioconjugated IONP clearance from the brain (Figures 4 and 5).

Histopathological analysis was performed on brain slices harvested from all the animals 30 days after their CED procedure. In all dogs, histopathological changes were localized to the catheter tracts. Gemistocytic astrocytosis and gitter cells (phagocytizing microglia) were found surrounding the CED catheter sites (Figure 6). Neovascularization and perivascular lymphoplasmacytic infiltration also were found around the catheter tracts. The presence of Fe-containing particles in the brain tissue was confirmed by Perl blue iron staining (Figure 6). Furthermore, both the astrocytes and microglia contained small spherical iron-positive particles (Figure 6), indicating the uptake and clearance of the IONPs from the brain by astrocytes and microglia.

DISCUSSION

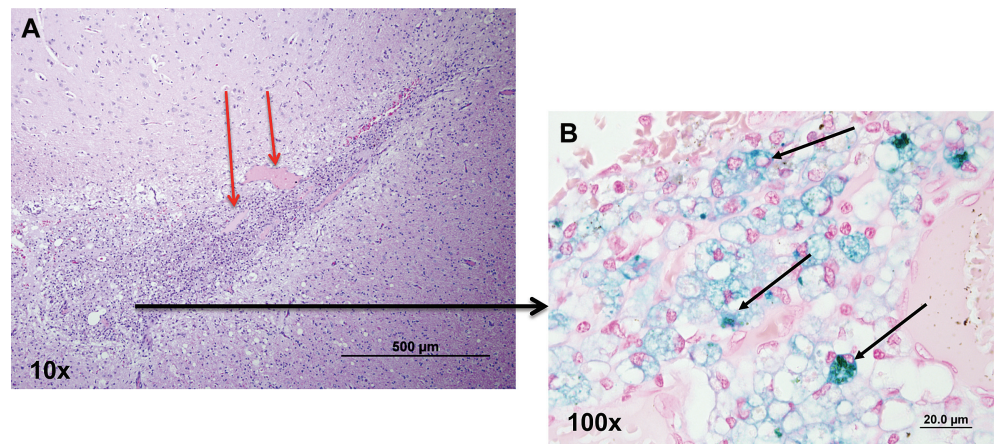
The CED of therapeutic agents into the brain remains a promising strategy for treating GBM. The ability to directly infuse high concentrations of agents both intratumorally and peritumorally where infiltrating cancer cells reside is a main treatment advantage with CED. Current systemic treatment strategies of GBM are unable to target tumors in a concentration high enough to prevent recurrence with acceptable systemic toxicity. Furthermore, targeting infiltrating cancer cells of GBMs outside the main tumor mass where the blood-brain barrier is intact is unsuccessful with any systemic therapy.

The inability to accurately define the extent and location of CED infusions has led to criticism of this treatment approach for GBMs and has compromised the efficacy data of the human clinical trials that have been performed.¹ Leakage of infusate into the ventricular or subarachnoid spaces can result in suboptimal tumor targeting and treatment failure.⁶

The use of real-time MRI has recently been described during intratumoral CED of liposomal nanoparticles containing the topoisomerase inhibitor CPT-11 and the surrogate marker gadoteridol into spontaneous gliomas in the canine¹⁴ and into the healthy canine brain.²² Volume of distribution of the infusate, cannula location, and leakage of infusate were determined by real-time MRI. With the real-time MRI approach, canine patients were placed in a stereotactic head frame while under general anesthesia and underwent CED for up to 4 hours while in the MRI scanner. The coinjection of gadoteridol permits immediate infusion distribution assessment and correlation to the treatment agent CPT-11. The MRI contrast effect of the gadoteridol is lost, however, shortly after CED.

Magnetic IONPs have recently been used for CED in rodent models.^{17,18,23} The ability to directly image these nanoparticles sensitively with MRI on T2WI and their ability to be covalently conjugated to tumor-specific therapeutic agents provide the basis for their use in CED and direct tumor targeting.¹⁸ Because of their size (10-nm core), cell endocytosis and penetration of IONPs through the extracellular matrix in the brain are possible.^{8,18,24} We have found that IONPs conjugated to an EGFRvIII antibody can distribute well after CED both intratumorally and peritumorally in human GBM xenografts implanted in rodents and can increase overall animal survival.¹⁷ The IONPs remain in the rodent brain for

FIGURE 6. Histopathologic analysis of the catheter tract in the canine brain 30 days after iron-oxide nanoparticle (IONP) convection-enhanced delivery (CED). A, hematoxylin and eosin-stained brain section of the CED catheter site surrounded by gitter cells (phagocytizing microglia; $\times 10$). Neovascularization is also seen (red arrows). B, magnified view ($\times 100$) revealing the presence of iron-filled gitter cells (black arrows) after Perl blue staining of brain section.



weeks after CED and continue to disperse into the normal brain days after CED, potentially targeting the infiltrating GBM cells that reside outside of the main tumor mass.¹⁷

All of our canine subjects required general anesthesia during the single CED catheter implantation into the brain and during MRI scanning after IONP CED. Each external programmable CED pump was strapped onto the canine subject after being connected to a subcutaneously tunneled catheter (Figure 2). The CED studies were performed on our awake canine subjects for up to 24 hours, and sensitive MRI monitoring of IONP distribution was possible up to 30 days later. Although MRI scans were performed on each subject at the completion of each CED procedure, the use of the Medtronic Synchronised II pump could permit MRI scanning during the CED procedure because it is MRI compatible for real-time CED imaging if needed. These pumps have been used for human intrathecal infusions and in a prior human GBM CED trial.¹

Using higher infusion rates (1, 3, or 5 $\mu\text{L}/\text{min}$) resulted in leak-back along the CED catheter of the IONPs with CED as confirmed by MRI (Figure 3). Our ability to directly image the IONPs by MRI revealed subarachnoid and intraventricular IONP distribution in two of our canine subjects (Figure 3). Although only 2 canines underwent a CED infusion rate of 0.5 $\mu\text{L}/\text{min}$, we found that this rate of infusion resulted in the best distribution of the IONPs in both the gray and white matter of the brain in the 2 canines tested (Figure 4). Dispersion at this rate was also found 5 days after the CED procedure (Figure 5).

All of our canine subjects showed no signs of toxicity or neurological deficits by clinical examination and hematologic and cerebrospinal fluid analyses after IONP CED. Predominant clearance of the bioconjugated cetuximab-IONPs was found at 30 days after CED. The accumulation of iron-filled gitter cells and gemistocytic astrocytes around each catheter site provided evidence for the uptake and clearance of the free and bioconjugated IONPs in the canine brain (Figure 6).

CONCLUSIONS

We have demonstrated for the first time the CED of magnetic IONPs into the healthy canine brain for distribution/

dispersion volume, clearance, and toxicity evaluation. Both free IONPs and cetuximab-conjugated IONPs were used in our canine subjects and could be sensitively monitored by MRI for days after CED. All of our canine subjects showed no signs of central nervous system or systemic toxicities after CED treatment. We believe bioconjugated cetuximab-IONPs represent a potential therapeutic agent that could be evaluated in canine patients with spontaneous gliomas after CED. The canine spontaneous glioma model represents one of the best models to study the delivery and efficacy of potential therapeutic agents that could be translated to human GBM patients.

Disclosure

This work was supported in part by grants from the National Institutes of Health (NS053454 to Dr Hadjipanayis, P50CA128301-01A10003 to Drs Mao and Hadjipanayis, 1U01CA151810-01 to Dr Mao, 5R01CA154846-02 to Dr Mao), the Georgia Cancer Coalition, Distinguished Cancer Clinicians and Scientists Program (to Dr Hadjipanayis), and the Dana Foundation (to Dr Hadjipanayis). The authors have no personal financial or institutional interest in any drugs, materials, or devices described in this article.

Acknowledgment

We would like to thank the Bioimaging Research Center as well as the pathology team at the University of Georgia College of Veterinary Medicine.

REFERENCES

- Kunwar S, Prados MD, Chang SM, et al. Direct intracerebral delivery of cintredekin besudotox (IL13-PE38QQR) in recurrent malignant glioma: a report by the Cintredekin Besudotox Intraparenchymal Study Group. *J Clin Oncol.* 2007;25(7):837-844.
- Mardor Y, Roth Y, Lidar Z, et al. Monitoring response to convection-enhanced taxol delivery in brain tumor patients using diffusion-weighted magnetic resonance imaging. *Cancer Res.* 2001;61(13):4971-4973.
- Bobo RH, Laske DW, Akbasak A, Morrison PF, Dedrick RL, Oldfield EH. Convection-enhanced delivery of macromolecules in the brain. *Proc Natl Acad Sci U S A.* 1994;91(6):2076-2080.
- Allard E, Passirani C, Benoit JP. Convection-enhanced delivery of nano-carriers for the treatment of brain tumors. *Biomaterials.* 2009;30(12):2302-2318.

5. Lidar Z, Mardor Y, Jonas T, et al. Convection-enhanced delivery of paclitaxel for the treatment of recurrent malignant glioma: a phase I/II clinical study. *J Neurosurg.* 2004;100(3):472-479.
6. Sampson JH, Archer G, Pedain C, et al. Poor drug distribution as a possible explanation for the results of the PRECISE trial. *J Neurosurg.* 2010;113(2):301-309.
7. MacKay JA, Deen DF, Szoka FC Jr. Distribution in brain of liposomes after convection enhanced delivery; modulation by particle charge, particle diameter, and presence of steric coating. *Brain Res.* 2005;1035(2):139-153.
8. Neeves KB, Sawyer AJ, Foley CP, Saltzman WM, Olbricht WL. Dilation and degradation of the brain extracellular matrix enhances penetration of infused polymer nanoparticles. *Brain Res.* 2007;1180:121-132.
9. Vavra M, Ali MJ, Kang EW, et al. Comparative pharmacokinetics of ¹⁴C-sucrose in RG-2 rat gliomas after intravenous and convection-enhanced delivery. *Neuro Oncol.* 2004;6(2):104-112.
10. Chen MY, Hoffer A, Morrison PF, et al. Surface properties, more than size, limiting convective distribution of virus-sized particles and viruses in the central nervous system. *J Neurosurg.* 2005;103(2):311-319.
11. Sampson JH, Brady ML, Petry NA, et al. Intracerebral infusate distribution by convection-enhanced delivery in humans with malignant gliomas: descriptive effects of target anatomy and catheter positioning. *Neurosurgery.* 2007;60(2 suppl 1):ONS89-ONS98; discussion ONS98-ONS99.
12. Varenika V, Dickinson P, Bringas J, et al. Detection of infusate leakage in the brain using real-time imaging of convection-enhanced delivery. *J Neurosurg.* 2008;109(5):874-880.
13. Saito R, Bringas JR, McKnight TR, et al. Distribution of liposomes into brain and rat brain tumor models by convection-enhanced delivery monitored with magnetic resonance imaging. *Cancer Res.* 2004;64(7):2572-2579.
14. Dickinson PJ, LeCouteur RA, Higgins RJ, et al. Canine spontaneous glioma: a translational model system for convection-enhanced delivery. *Neuro Oncol.* 2010;12(9):928-940.
15. Sampson JH, Akabani G, Archer GE, et al. Intracerebral infusion of an EGFR-targeted toxin in recurrent malignant brain tumors. *Neuro Oncol.* 2008;10(3):320-329.
16. Sampson JH, Akabani G, Friedman AH, et al. Comparison of intratumoral bolus injection and convection-enhanced delivery of radiolabeled antitenascin monoclonal antibodies. *Neurosurg Focus.* 2006;20(4):E14.
17. Hadjipanayis CG, Machaidze R, Kaluzova M, et al. EGFRvIII antibody-conjugated iron oxide nanoparticles for magnetic resonance imaging-guided convection-enhanced delivery and targeted therapy of glioblastoma. *Cancer Res.* 2010;70(15):6303-6312.
18. Wankhede M, Bouras A, Kaluzova M, Hadjipanayis CG. Magnetic nanoparticles: an emerging technology for malignant brain tumor imaging and therapy. *Expert Rev Clin Pharmacol.* 2012;5(2):173-186.
19. Stoica G, Kim HT, Hall DG, Coates JR. Morphology, immunohistochemistry, and genetic alterations in dog astrocytomas. *Vet Pathol.* 2004;41(1):10-19.
20. Dickinson PJ, Roberts BN, Higgins RJ, et al. Expression of receptor tyrosine kinases VEGFR-1 (FLT-1), VEGFR-2 (KDR), EGFR-1, PDGFRalpha and c-Met in canine primary brain tumours. *Vet Comp Oncol.* 2006;4(3):132-140.
21. Higgins RJ, Dickinson PJ, LeCouteur RA, et al. Spontaneous canine gliomas: overexpression of EGFR, PDGFRalpha and IGF2 demonstrated by tissue microarray immunophenotyping. *J Neurooncol.* 2010;98(1):49-55.
22. Dickinson PJ, LeCouteur RA, Higgins RJ, et al. Canine model of convection-enhanced delivery of liposomes containing CPT-11 monitored with real-time magnetic resonance imaging: laboratory investigation. *J Neurosurg.* 2008;108(5):989-998.
23. Perlstein B, Ram Z, Daniels D, et al. Convection-enhanced delivery of maghemite nanoparticles: increased efficacy and MRI monitoring. *Neuro Oncol.* 2008;10(2):153-161.
24. Thorne RG, Nicholson C. In vivo diffusion analysis with quantum dots and dextrans predicts the width of brain extracellular space. *Proc Natl Acad Sci U S A.* 2006;103(14):5567-5572.